Korean J. Chem. Eng., 34(7), 2099-2109 (2017)
DOI: 10.1007/s11814-017-0102-5

pISSN: 0256-1115
eISSN: 1975-7220

Optimization and analysis of reaction injection molding of polydicyclopentadiene using response surface methodology

Hyeon-Gook Kim, Hye Jeong Son, Dong-Koo Lee, Dong-Woo Kim, Hye Jin Park, and Deug-Hee Cho†

Chemical Industry Development Center, Korea Research Institute of Chemical Technology,
45, Jongga-ro, Jung-gu, Ulsan 44412, Korea
(*Received 2 November 2016 • accepted 5 April 2017*)

Abstract−Reaction injection molding (RIM) process conditions for polydicyclopentadiene (PolyDCPD) were optimized by using a Box-Behnken design (BBD) from the response surface methodology (RSM). The RIM process parameters, such as smoke time, exotherm time, highest exotherm and PolyDCPD conversion, were tuned by changing the variables (the amount of catalyst, cocatalyst and moderator). Under the optimized condition, the ring-opening metathesis polymerization reaction of dicyclopentadiene did not occur within 100 s, the maximum temperature was reached within 4 min, and the polydicyclopentadiene conversion was over 98%. Therefore, dicyclopentadiene could be safely put into the mold in a total cycle time of less than 6 min and produce PolyDCPD with mechanical properties sufficient for industry applications.

Keywords: Polydicyclopentadiene, Dicyclopentadiene, Ring-opening Metathesis, Box-Behnken Design, Reaction Injection Molding

INTRODUCTION

As a solution to reduce automotive exhaust gas and enhance fuel efficiency, lightweight vehicles are important in the automotive industry. When the vehicle weight is 10% lower, fuel consumption is reduced by 7% [1]; consequently, automakers worldwide have increased their investment in lighter vehicles [2]. This vehicle weight reduction could be achieved using low-density materials, such as aluminum, magnesium, and plastics, instead of steel [2]. Among them, the use of plastics in car exteriors is surging because of their flexibility in manufacture, lighter specific gravity, and durability. Petrochemical by-products have been applied to take advantage of this new investment in the automotive industry [3]. DCPD can be extracted from the C5 fraction in 15-20% yield and the applications are diverse, depending on its purity [4-9]. Low purity (80%) DCPD is used in unsaturated polyester resin, hydrocarbon resins; high purity (95%) DCPD is used in ethylidene norbornene (ENB), ethylene propylene diene monomer (EPDM), cyclic olefin polymers (COP) and copolymers (COC). Ultrapure DCPD (99%>) is used in Polydicycopentadiene (PolyDCPD); however, it occupies only 4% in DCPD application [10-14]. According to 2013 data from NexantThinking, global DCPD production increased steadily from approximately 500,000 tons in 2000 to about 800,000 tons in 2012, with demand showing a similar increase [15]. If more ultrapurity DPCD is applied to the car industry as PolyDCPD, the value of the DCPD increases. The world PolyDCPD market in 2015 was estimated to be $715 million (about 8,200 million) [16,17]. The US, Japan, and Europe are the main producers and consumers of PolyDCPD due to the availability of advanced technologies. Leading PolyDCPD manufacturers include Romeo RIM (US), Polirim (Italy), Wanyard (Germany), and Osborne Industries (USA) [16, 17]. Zeon Corporation (Japan) merged with Teijin Metton whose Molding Network and established a joint venture company, RIM-TEC Corporation to achieve vertical integration, from raw materials to PolyDCPD RIM molding products and expand their marketing offensive for a greater global market share [16,18]. Sojitz incorporated Cymetech, a DCPD production company in 2008 and Metton America, a Metton resin producer in 2014 as a subsidiary and produced truck bumpers and bonnets/hoods as an alternative to unsaturated polyester by developing a high-stiffness grade [19,20].

The DCPD structure combines those of norbornene and cyclopentene, and is used as raw material in the preparation of cross-linked-type cyclo-olefin thermoplastic resin, polyDCPD shown in Scheme 1. [17-20]. PolyDCPD is generated by ring-opening metathesis polymerization (ROMP) of the double bond in the norbornene portion using a catalyst [25-27]. The network structure is then generated by cross-linked cyclopentene double bonds formed during exothermic ring opening reaction [25,26,28]. In 1995, PolyDCPD using reaction injection molding (RIM) process was commercialized and used in car hoods, truck parts, and agricultural tractors [29-31]. Since then, PolyDCPD has been applied in the transport (vehicle body panels), construction machinery (excavators), chem-

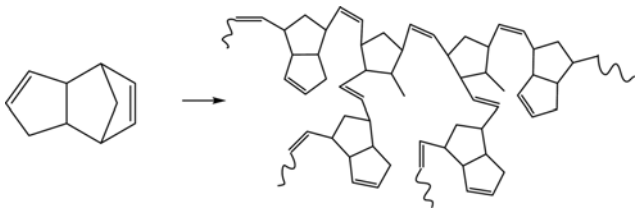

Scheme 1. PolyDCPD network by ring-opening metathesis of DCPD.

†To whom correspondence should be addressed.
E-mail: dhcho@krict.re.kr

ical (Chlor-Alkali containers), agricultural, and medical industries, as well as in sporting goods and military equipment [28,32]. PolyDCPD has excellent impact and bending strengths, with the unique feature of high impact resistance at low temperatures [27,33,34]. Furthermore, its excellent adhesion could be applied in coating materials [32,35-37]. PolyDCPD is about half the density (1.03 cc/g) of sheet molding composite (SMC) used in some automotive plastics and is lighter than polycarbonate (PC), polyamide (PA) considered as a material in the production of light vehicles [17]. The introduction of electric vehicles presents new challenges in reducing vehicle weight [38]. Among them, technical constraints, particularly the low-energy density batteries, require a considerable reduction in vehicle weight [38]. Solutions have been sought through the development of new materials and design of new assembly method configurations [38]. Currently, the energy density of a Li-ion battery is 190 Wh/kg, which is dependent on vehicle weight. DCPD RIM technology will be necessary to reduce vehicle weight, which should not exceed 400 kg without the battery [38]. In the future, DCPD demand in the automotive industry is expected to enhance DCPD market growth [17,39].

We conducted experiments using response surface methodology (RSM) and interpreted the data by controlling the content of the catalyst, cocatalyst, stabilizer, and moderator in the RIM process for PolyDCPD. With the electric car era approaching, the importance of PolyDCPD is increasing. Until now, no research has been conducted on the variables affecting the RIM process using RSM. Although there are patents optimized [40] through several experiments, we believe RSM analysis is necessary for using more accurate parameter values. With this research, we hope to use these PolyDCPD with excellent physical properties developed through RSM analysis in the application of electric car exterior to replace other plastics and steel.

MATERIALS AND METHODS

1. Chemicals and Reagents

The homopolymerization of the purified DCPD is catalyzed by a two-part metathesis-catalyst system. One part (Solution A) contains a tungsten containing catalyst, such as a tungsten halide or tungsten oxyhalide, preferably WCl_6 or $WOCl_4$ [40]. The other part (Solution B) contains an activator such as an alkylaluminum compound. The tungsten compound, if unmodified, will rapidly polymerize the monomer. Consequently, the tungsten compound should first be suspended in a small amount of a suitable solvent. Examples of preferred solvents are benzene, toluene, chlorobenzene, dichlorobenzene, and trichlorobenzene [40]. To prevent premature polymerization of the tungsten compound/monomer solution, Lewis base or a chelating agent can be added. Preferred Lewis bases are nitriles and ethers such as benzonitrile and tetrahydrofuran. An unmodified activator/monomer solution is mixed with the catalyst/monomer solution, the polymerization would initiate instantaneously and the polymer could set up in the mixing head [40]. The onset of polymerization can be delayed by adding a moderator to the activator/monomer solution. Ethyl benzoate and butyl ether are most preferred [40]. The ROMP mechanism of WCl_6 and Et_2AlCl is catalyzed with cocatalyst to activate W-carbene species (W-alkylidene) [41]. And then the coordination of the olefin of DCPD onto the metal atom of this species, followed by the shift of the coordinated olefin to form the metallocyclobutane intermediate, and finally the topologically identical shift of the new coordinated olefin in the metallocyclobutane in a direction perpendicular to the initial olefin shift [41].

DCPD (95%) was obtained from Acros Organics (Geel, Belgium). Polybutadiene (Mw=200,000). Tungsten hexachloride (WCl_6, >99.99%), benzonitrile (anhydrous, >99%), toluene (anhydrous, 99.8%), diethylaluminum chloride (Et_2AlCl, 1.0 M in hexanes), di-*n*-butyl ether (anhydrous, 99.3%), and *p*-tert-butylphenol (99%) were purchased from Sigma-Aldrich (St. Louis, MO, USA).

2. Preparation of PolyDCPD

Since metal alkylidenes are too reactive or can be unstable at the required molding temperatures, RIM-ROMP processes depend on in situ generation of the active metathesis catalyst by combining a procatalyst (Solution A) with a cocatalyst (Solution B), which are mixed just before being injected into the mold [42,43]. The active catalyst, presumably a metal alkylidene or metalacyclobutane, is formed and polymerization occurs within a few minutes [42].

All experiments were conducted in a glove box with moisture and oxygen content below 10 ppm. DCPD was put under a high vacuum at room temperature for 12 h to remove water and trace cyclopentadiene. Polybutadiene (5 wt%) was dissolved in DCPD completely after water was removed under high vacuum. Other chemicals were used directly without any treatment. The catalyst solution was prepared by dissolving WCl_6 (18.83 g, 0.05 mol) in toluene (46.07 g, 0.5 mol) and *p*-tert-butylphenol (7.511 g, 0.05 mol) over 24 h, before adding benzonitrile (5.1556 g, 0.05 mol) as a stabilizer. Solution A was prepared by adding the catalyst solution to DCPD (5 wt% polybutadiene) over 1 min. Solution B was prepared by adding Et_2AlCl, as the cocatalyst, and di-*n*-butylether, as the moderator, to stirred DCPD (5 wt% polybutadiene) over 1 min. Solutions A and B were combined on an aluminum plate maintained at 60 °C and stirred at 800 rpm to prepare PolyDCPD. Tensile, flexural, and impact strength specimens were prepared using the following procedure: After stirring Solution A and Solution B for 1 min, we poured them into a standard mold and kept at 60 °C in the oven under a nitrogen atmosphere for 10 min, before aging at 100 °C for 1 h.

3. Characterization

The initial gel time, smoke time and exotherm time were measured with a timer, and the exotherm temperature was determined with a thermometer. PolyDCPD conversion was measured by thermogravimetric analysis (TGA Q500, TA Instruments) from room temperature to 800 °C. Tensile strength was measured by using a universal testing machine (UTM 5982, Instron Co.) using a 3.2 mm thick specimen at a crosshead speed of 50 mm/min. The tensile strength and elastic modulus were calculated by dividing the force measured during the tensile test by the unit cross section area of the sample. Sample preparation and measurement was performed according to standard method ASTM-D-638. The flexural strength of the sample was measured by using a three-point bending test according to standard method ASTM-D-790. The specimen size was 110 mm (width)×12.5 mm (height)×3.2 mm (thick-

ness). Furthermore, the test conditions were measured using a universal testing machine (UTM 5982, Instron Co.) at a crosshead speed of 50 mm/min. Impact strength was measured by Izod impact strength test (ASTM-D-256) by making an artificial V-shaped notch in the sample (63.5 mm (width)×12.5 mm (height)×6.4 mm (thickness). This test was conducted by hitting the notched specimen with a pendulum (2.084 kg) Impact strength was measured by obtaining the absorption energy, which was calculated from the height of pendulum rotation and the cross-sectional area at the notch.

4. Experimental Design for RSM

RSM is a collection of experimental strategies, mathematical methods, and statistical inference for constructing and exploring an approximate functional relationship between a response variable and a set of design variables [44]. The Box-Behnken design (BBD) is one of the most important and uncomplicated RSM designs. It requires fewer experiments than others, making it more economical to operate [45,46]. Design Expert software (Version 9.0, Stat-Ease, Inc., Minneapolis, MN) was used for experimental design, data analysis, and quadratic model building [47]. The mathematical relationship, involving a second-order polynomial model, used to estimate the effects of various factors on a response, is given by:

$$Y = l_0 + \Sigma_{i=1}^{3} l_i X_I + \Sigma_{i=1}^{3} l_i X_i^2 + \Sigma_{i=1}^{2} \Sigma_{j=i+1}^{3} l_{ij} X_i X_j \quad (1)$$

where Y is the response; λ_0, λ_i, λ_{ii}, and λ_{ij} are constant coefficients; and X is the actual (uncoded) value of the independent variable [48]. Using Eq. (1), we can evaluate the linear, quadratic, and interactive effects of independent variables on the response. The significance of the effect of the independent variables on the response was evaluated by of variance (ANOVA) through Fisher's test and shown by *p*-values below 0.05. The multiple correlation coefficients (R^2) and adjusted R^2 values were used as quality indicators for the fit of the second-order polynomial model equation [45,49]. Interactions between coded variables (–1, 0, 1) and response were shown using three-dimensional surface plots [48,49]. Response surfaces and contour plots are commonly used to evaluate relationships among parameters and predict results under given conditions [50]. The use of RSM not only allows the reduction of the number of experiments required to obtain the optimal values, but also enables the collection of more data that those calculated probabilistically. In this case, the number of experiments generally required can be at least 27 or much more. By using RSM, however, all data in a set of 15 experiments can be implemented as a 3D plot.

5. PolyDCPD Process Parameters

The response surfaces plots were applied for the PolyDCPD synthesis using the W catalyst system. Four RSM 3D plots using three parameters were constructed for the PolyDCPD additives formulation. In addition, alteration of two variables was described while keeping one variable at its mean level. The interaction between the corresponding variables can be disregarded when the contour of the response surface is circular. However, it is important to consider the interactions between the relevant variables for an elliptical contour response surface [51]. The PolyDCPD RIM molding process proceeds in the following order: One DCPD solution containing elastomer catalyst and stabilizer (Solution A), and the other DCPD solution containing elastomer, cocatalyst and moderator (Solution B), are injected into the mold in a 1 : 1 ratio after being uniformly mixed in a mixing head at a pressure of 1,500-3,000 psi [52-55]. The injected mixture is cured at the reaction temperature in the mold within about 360 s to give the completed product. The reactivity of the two components injected into the mixing head is very important. If the amounts of catalyst (curing agent) and cocatalyst (activator) are high, curing will start before the mixture enters the mold, so the product cannot be obtained. Conversely, if the amounts of curing agent and activator are less, curing will not occur, even after injection into the mold, which again would result in no product. Therefore, adjusting the compositions of both liquids in RIM molding is important for controlling curing time and cross-link density. In the DCPD RIM process, the process response includes smoke time, exotherm time, highest exotherm, and PolyDCPD conversion. When the DCPD polymerization reaction starts, the time taken for smoke to be generated is the smoke time, which means the time taken for the reaction temperature to first rise due to exothermic reaction. If these responses are too fast, it is difficult to prepare the desired products because the polymerization occurs before entering the mold, while if they are too slow, the cycle time increases. When DCPD is reacted in the mold, the maximum reaction temperature reached is called the exotherm temperature and the time taken to reach the highest temperature is called exotherm time. PolyDCPD conversion is the ratio of complete reacted DCPD to the total injected DCPD, which should be 98% or higher. For PolyDCPD, if the process cycle time is known to be about 6 min, the exotherm time should be about 4 min. In the exothermic reaction, the highest exotherm should be more than 190 °C when the reaction is complete. If lower, unreacted DCPD would remain in PolyDCPD, resulting in poor mechanical properties. The smoke time should be more than 100 s. Accordingly, the optimum response conditions for PolyDCPD RIM molding are shown in Table 1 where the four responses (Y) are smoke time (s), initial heating time (s), exotherm time (s), exotherm temperature (°C) and PolyDCPD conversion (%). The three independent variables were the DCPD to catalyst molar ratio (A), the DCPD to cocatalyst molar ratio (B), and the DCPD to moderator (C), as shown in Table 2 and in the level of the low (–1), middle (0) and high (+1) of each variable were

Table 1. Process response and their optimum ranges for DCPD reaction injection molding process

Process response (Y)	Optimum range
Smoke time (s)	100-180
Exotherm time (s)	180-240
Highest exotherm (°C)	>190
PolyDCPD Conversion (%)	>8

Table 2. Coded levels for independent factors in DCPD RIM used in the Box-Behnken design

Independent factors	Symbol	Coded levels		
		−1	0	1
Catalyst/DCPD molar ratio	A	3000	2000	1000
Cocatalyst/DCPD molar ratio	B	1000	500	250
Moderator/DCPD molar ratio	C	800	400	100

Table 3. Box-Behnken experimental designs for independent variables in PolyDCPD composition and their response values for DCPD RIM process

	Factors			Smoke time (s)	Exotherm time (sec)	Exotherm temperature (°C)	PolyDCPD conversion (%)
	A	B	C				
1	3000	1000	400	261	301	203.8	98.7
2	1000	1000	400	209	276	230.4	97.7
3	3000	250	400	25	84	107.2	85.9
4	1000	250	400	7	41	157.2	86.2
5	3000	500	800	90	152	143.5	95.4
6	1000	500	800	25	80	155	90.4
7	3000	500	100	197	259	172.3	93.1
8	1000	500	100	60	116	193.1	97.6
9	2000	1000	800	226	278	210	97.9
10	2000	250	800	17	80	131.1	89.9
11	2000	1000	100	240	274	212.3	98.1
12	2000	250	100	30	72	139.2	90.0
13	2000	500	400	80	119	169.1	94.3
14	2000	500	400	69	99	158	93.8
15	2000	500	400	60	113	176.8	96.2

Table 4. Analysis of variance (ANOVA) for response surface model of smoke time

Source		Sum of squares	df	Mean square	F-value	P-value (Prob>F)
Model	114300.00	6	19048.13	30.64	<0.0001	Significant
Catalyst (A)	9248.00	1	9248.00	14.87	0.0048	
Cocatalyst (B)	91806.13	1	91806.13	147.65	<0.0001	
Moderator (C)	3570.13	1	3570.13	5.74	0.0434	
AC	1296.00	1	1296.00	2.08	0.1868	
B^2	7958.31	1	7958.31	12.80	0.0072	
C^2	706.17	1	706.17	1.14	0.3177	
Residual	4974.17	8	621.77			
Lack of fit	4693.51	6	782.25	5.57	0.1599	Not significant
Pure error	280.67	2	140.33			
Cor. total	119300.00	14				

R-squared=0.9583, Adj R-squared=0.9270, Pred R-squared=0.7461, Adeq precision=16.623

designated [50]. A total of 15 experiments, including 12 factorial points and three replicates at the center point for the estimation of the pure error sum of squares, were performed based on the Box-Behnken design matrix generated by Design Expert software [45]. The responses of these 15 experiments are shown in Table 3.

RESULTS AND DISCUSSION

The 3D plots in Fig. 1-4 represent the expression of the four different response values, which should be in the optimum ranges shown in Table 1. In each figure, there is a section in the response range corresponding to a change in the combination of catalyst, cocatalyst, stabilizer, and regulator. The combination that satisfies each response interval becomes the optimal range. To obtain this, each range was checked with a 3D plot using BBD, and finally, the optimal combination satisfying all 3D response ranges was obtained using an optimization program.

1. Smoke Time

Table 4 shows the results of ANOVA for smoke time. The model F-value of 30.64 implies that the model was significant. There was only a 0.01% chance that an F-value this large could be due to noise. Values of Prob>F less than 0.0500 indicate that the model terms are significant. In this case A, B, C, and B^2 were significant model terms. The lack of fit F-value of 5.57 implies that the lack of fit was not significant relative to the pure error, with a 15.99% chance that such a large lack of fit F-value could be due to noise. The Pred. R-Squared value of 0.7461 was in reasonable agreement with the Adj. R-Squared value of 0.9270, because the difference was less than 0.2. Adeq. Precision measures the signal-to-noise ratio, for which a value greater than 4 is desirable. The ratio of 16.623 indicated an adequate signal, meaning that this model could be used to navigate the design space. All linear coefficients of the catalyst (A), cocatalyst (B), moderator (C), and the quadratic term of cocatalyst^2 (B^2) were significant. The response surface and contour curves were

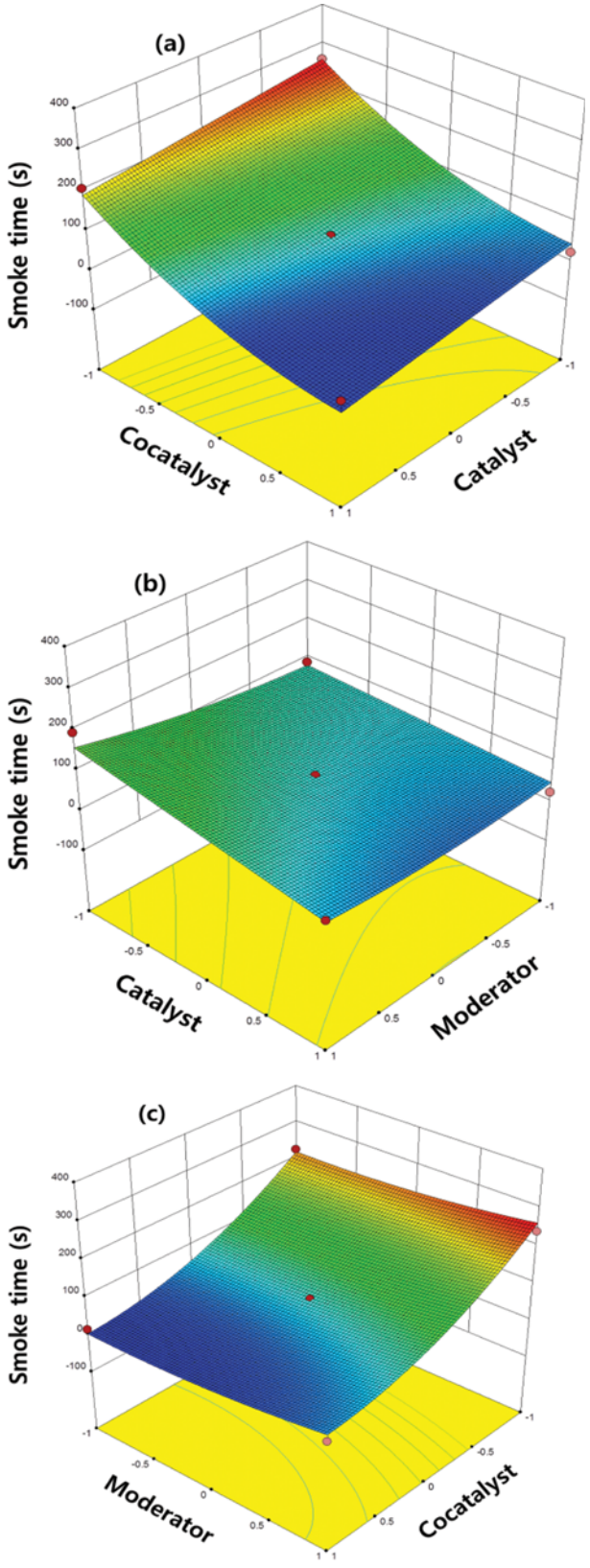

Fig. 1. Response surface plot of smoke time in the DCPD RIM process (a) with constant moderator (coded level=0, DCPD/moderator=400), (b) with constant cocatalyst (coded level=0, DCPD/cocatalyst=500), and (c) with constant catalyst (coded level=0, DCPD/catalyst=2000).

obtained using following Eq. (2):

$$\text{Smoke time} = +73.69 - 34.00\times\text{Catalyst} - 107.13\times\text{Cocatalyst} + 21.13\times\text{Moderator} - 18.00\times\text{Catalyst}\times\text{Moderator} + 46.29\times\text{Cocatalyst}^2 + 13.79\times\text{Moderator}^2 \quad (2)$$

This equation can be interpreted as the catalyst and cocatalyst having a negative effect, and the moderator having a positive effect, on smoke time, with the square of the cocatalyst also being related to smoke time. The catalyst and moderator interacted with each other in relation to smoke time. Fig. 1(a) shows how the amount of catalyst and cocatalyst affected the smoke time with constant moderator. The smoke time was shorter when using larger amounts of catalyst and cocatalyst. This means that the ROMP reaction both started and gelled faster. Therefore, an appropriate response delay time was acquired by controlling the amount of catalyst and the cocatalyst in the DCPD RIM process. The catalyst had a minimal impact on the smoke time, while the large impact of cocatalyst can be seen. The smoke time was adjusted from 0 s to 190 s when the catalyst was 1 (DCPD/catalyst=1000, see Table 2) in accordance with the cocatalyst content, and was also adjustable from 40 s to 260 s when the catalyst was −1 (DCPD/catalyst=3000) according to the cocatalyst content. Fig. 1(b), (c) shows the effect of moderator on smoke time. In Fig. 1(b) smoke time increased from 82 s to 89 s as the moderator increases when the catalyst was −1 (DCPD/catalyst=3000) and increased from 82 s to 157 s when catalyst was 1 (DCPD/catalyst=1000). In Fig. 1(b) the catalyst and the moderator interact with each other as mentioned in Eq. (1). When the amount of catalyst is small (catalyst ~−1), there is almost no change in smoke time despite change in the moderator content. However, when the amount of catalyst is large, the amount of moderator becomes small (~−1), and the smoke time becomes longer (~150 s). In Fig. 1(c) smoke time increased from 5 s to 47 s as the moderator increased when cocatalyst was −1 (DCPD/cocatalyst=1000) and increased from 220 s to 260 s when cocatalyst was 1 (DCPD/cocatalyst=250).

2. Exotherm Time

Table 5 shows the ANOVA results for exotherm time. The F-value of 19.71 implies that the model was significant. The Prob>F values of A, B, and B^2 show them to be significant model terms. The lack of fit F-value of 11.69 had only an 8.09% of being due to noise. The Pred. R-Squared value of 0.7497 was in reasonable agreement with the Adj. R-Squared of 0.8891. Signal-to-noise ratio was 13.478. The linear coefficients of the catalyst (A), cocatalyst (B), and the quadratic term of cocatalyst^2 (B^2) were significant. The response surface and contour curves were obtained using Eq. (3):

$$\text{Exotherm time} = +110.33 - 35.38\times\text{Catalyst} - 106.50\times\text{Cocatalyst} + 16.38\times\text{Moderator} + 20.46\times\text{Catalyst}^2 + 44.701\times\text{Cocatalyst}^2 + 20.96\times\text{Moderator}^2 \quad (3)$$

where the catalyst and cocatalyst can be interpreted as having a negative effect on time to exotherm and the square of the cocatalyst was related to the time to exotherm. In Eq. (3), no interaction occurs between the variables. Fig. 2(a) shows how the amounts of catalyst and cocatalyst affected the time to reach a maximum temperature with constant moderator. The more catalyst and cocatalyst, the faster the maximum temperature is reached. A fast exotherm

Table 5. Analysis of variance (ANOVA) for response surface model of exotherm time

Source	Sum of square	df	Mean square	F-value	P-value (Prob>F)	
Model	112300.00	6	18723.79	19.71	0.0002	Significant
Catalyst (A)	10011.13	1	10011.13	10.54	0.0118	
Cocatalyst (B)	90738.00	1	90738.00	95.54	<0.0001	
Moderator (C)	2145.13	1	2145.13	2.26	0.1713	
A^2	1545.39	1	1545.39	1.63	0.2379	
B^2	7380.31	1	7380.31	7.77	0.0236	
C^2	1621.85	1	1621.85	1.71	0.2276	
Residual	7598.17	8	949.77			
Lack of fit	7387.50	6	1231.25	11.69	0.0809	Not significant
Pure error	210.67	2	105.33			
Cor. total	119900.00	14				

R-squared=0.9367, Adj R-squared=0.8891, Pred R-squared=0.7497, Adeq precision=13.478

Table 6. Analysis of variance (ANOVA) for response surface model of exotherm temperature

Source	Sum of squares	df	Mean square	F value	P-value (Prob>F)	
Model	15558.53	6	2593.09	20.91	0.0002	Significant
Catalyst (A)	1482.40	1	1482.40	11.95	0.0086	
Cocatalyst (B)	12944.41	1	12944.41	104.39	<0.0001	
Moderator (C)	746.91	1	746.91	6.02	0.0397	
AB	136.89	1	136.89	1.10	0.3241	
AC	21.62	1	21.62	0.17	0.6872	
B^2	226.30	1	226.30	1.83	0.2137	
Residual	992.02	8	124.00			
Lack of fit	697.04	6	116.17	0.79	0.6531	Not significant
Pure error	294.98	2	147.49			
Cor. total	16550.55	14				

R-squared=0.9401, Adj R-squared=0.8951, Pred R-squared=0.7253, Adeq precision=14.404

time results in faster ROMP completion, and so it is necessary for adjusting the reaction time in the DCPD RIM process. The exotherm time was adjusted from 50 s to 240 s when the catalyst was 1 (DCPD/catalyst=1000, see Table 2) in accordance with the cocatalyst content, and from 100 s to 320 s when the catalyst was −1 (DCPD/catalyst=3000) according to the cocatalyst content. In Fig. 2(b) exotherm time increased from 168 s to 200 s as the moderator increases when the catalyst was −1 (DCPD/catalyst=3000) and increased from 100 s to 120 s when catalyst was 1 (DCPD/catalyst=1000). In Fig. 2(c) exotherm time was increased from 264 s to 299 s as the moderator increase when cocatalyst was −1 (DCPD/cocatalyst=1000) and increased from 52 s to 85 s when cocatalyst was 1 (DCPD/cocatalyst=250)

3. Exotherm Temperature

Table 6 shows the ANOVA results for exotherm temperature. The model F-value of 20.91 implies the model was significant. The Prob>F values of A, B, and C show that they were significant model terms. The lack of fit F-value of 0.79 implies that the lack of fit was not significant relative to the pure error. The Pred. R-Squared of 0.7253 was in reasonable agreement with the Adj. R-Squared of 0.8951. Signal-to-noise ratio was 14.404. All linear coefficients of the catalyst (A), cocatalyst (B), and moderator (C) were significant. The response surface and contour curves were obtained using Eq. (4):

$$\begin{aligned}\textbf{Exotherm temperature} = {} & +166.11+13.61\times\text{Catalyst} \\ & -40.23\times\text{Cocatalyst}+9.66\times\text{Moderator} \\ & +5.85\times\text{Catalyst}\times\text{Cocatalyst}+2.32 \\ & \times\text{Catalyst}\times\text{Moderator}+7.762\times\text{Cocatalyst}^2\end{aligned} \quad (4)$$

where linear factors catalyst and moderator had a positive effect, and the cocatalyst had a negative effect, on exotherm temperature. The catalyst interacted with both cocatalyst and moderator in relation to the exotherm temperature. Fig. 3(a) shows how the amount of catalyst and cocatalyst affected the maximum temperature with constant moderator. When increasing catalyst amount, the exotherm temperature increased, and when increasing the cocatalyst amount, the exotherm temperature decreased. The exotherm temperature was increased up to 220 °C, which was beneficial because higher values allowed all DCPD to be involved in the ring opening exothermic reaction. The exotherm temperature was adjusted from 160 °C to 221 °C when the catalyst was 1 (DCPD/catalyst=1000, see Table 2), in accordance with the cocatalyst content, and from 107 °C to 208 °C when the catalyst was −1 (DCPD/catalyst=3000), in accordance with the cocatalyst content. The highest value

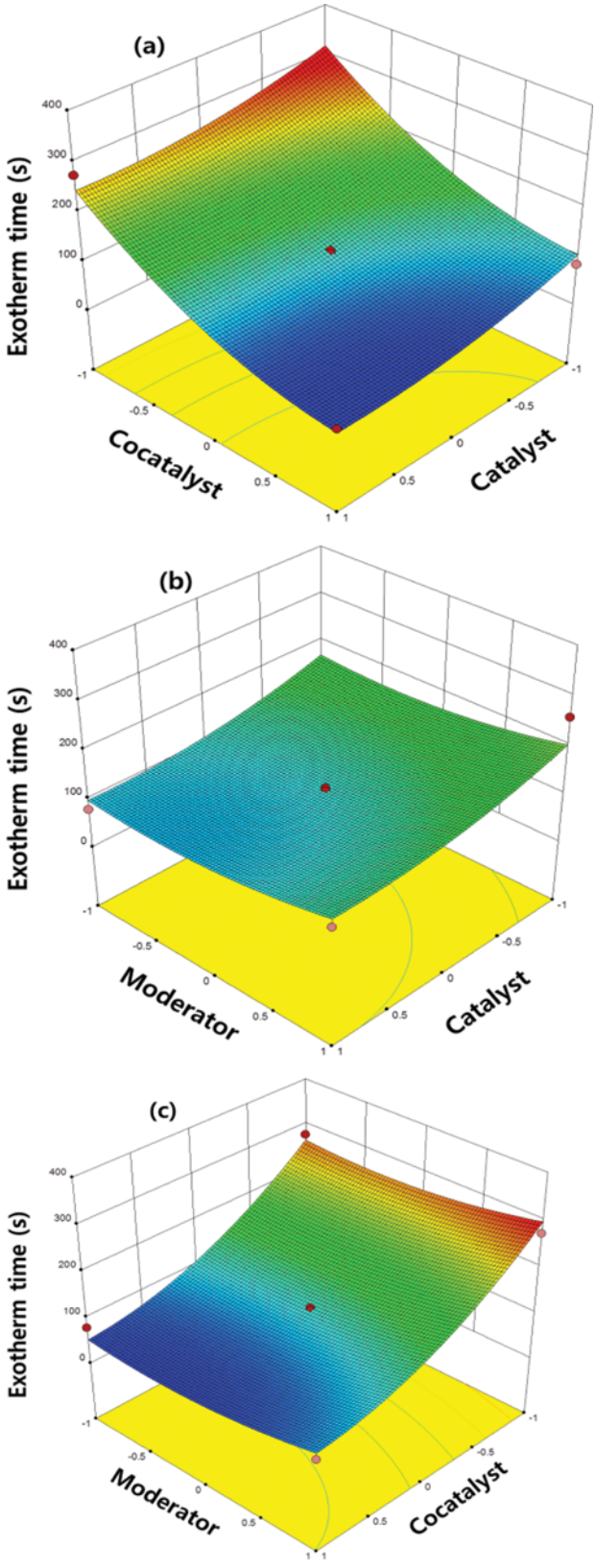

Fig. 2. Response surface plot of exotherm time in DCPD RIM process (a) with constant moderator (coded level=0, DCPD/moderator=400), (b) with constant cocatalyst (coded level=0, DCPD/cocatalyst=500, and (c) at constant catalyst (coded level=0, DCPD/catalyst=1000).

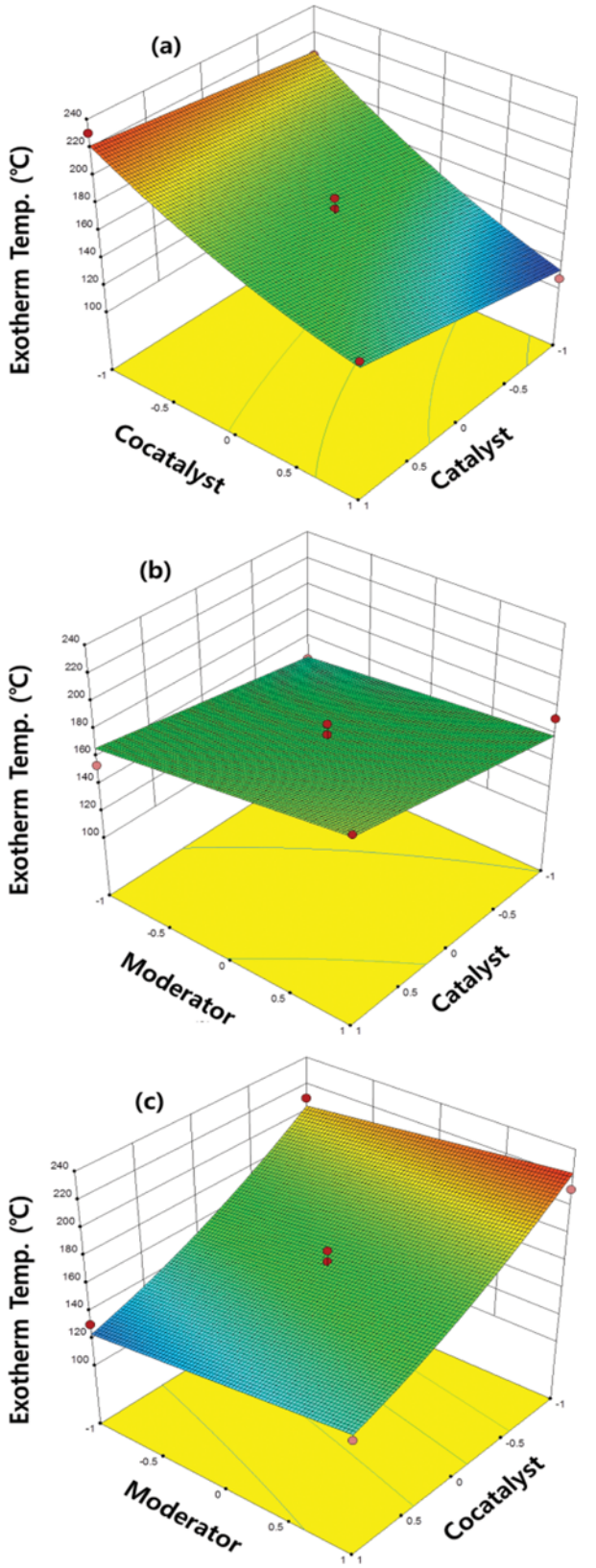

Fig. 3. Response surface plot of exotherm temperature in the DCPD RIM process (a) with constant moderator (coded level=0, DCPD/moderator=400), (b) with constant cocatalyst (coded level=0, DCPD/cocatalyst=500), and (c) with constant catalyst (coded level=0, DCPD/catalyst=1000).

Table 7. Analysis of variance (ANOVA) for response surface model of PolyDCPD conversion

Source	Sum of squares	df	Mean square	F value	P-value Prob>F	
Model	244.50	7	34.93	16.65	0.0007	Significant
A-Catalyst	0.18	1	0.18	0.086	0.7781	
B-Cocatalyst	204.02	1	204.02	97.24	<0.0001	
C-Moderator	3.38	1	3.38	1.61	0.2449	
AC	22.56	1	22.56	10.75	0.0135	
A^2	5.73	1	5.73	2.73	0.1424	
B^2	7.19	1	7.19	3.43	0.1065	
C^2	1.35	1	1.35	0.64	0.4492	
Residual	14.69	7	2.10			
Lack of fit	11.48	5	2.30	1.43	0.4598	Not significant
Pure error	3.21	2	1.60			
Cor total	259.18	14				

R-squared=0.9433, Adj R-squared=0.8867, Pred R-squared=0.7336, Adeq precision=12.053

of 221 °C and the conditions were (1, −1, 0); i.e., DCPD/catalyst= 1000, DCPD/Cocatalyst=1000, DCPD/Moderator=400. The catalyst and cocatalyst interact with each other in Fig. 3(a). In the presence of large amounts of catalyst (~1), the exotherm temperature increases less rapidly as the amount of cocatalyst decreases, while when the amount of the catalyst is small (~−1), the exotherm temperature increases more rapidly as the amount of the cocatalyst decreases. In Fig. 3(b) exotherm temperature increased from 145 °C to 159 °C as the moderator increased when the catalyst was −1 (DCPD/catalyst=3000) and increased from 165 °C to 185 °C when catalyst was 1 (DCPD/catalyst=1000). Therefore, the catalyst and the moderator also have an interaction with each other. In Fig. 3(c) exotherm temperature was increased from 203 °C to 222 °C as the moderator increases when cocatalyst was −1 (DCPD/cocatalyst=1000) and increased from 124 °C to 143 °C when cocatalyst was 1 (DCPD/cocatalyst=250)

4. PolyDCPD Conversion

Table 7 shows ANOVA results for PolyDCPD conversion. The model F-value of 16.65 implies the model was significant. The Prob>F values of B and AC show that they were significant model terms. The lack of fit F-value of 1.43 implies that the lack of fit was not significant relative to the pure error. The Pred. R-Squared value of 0.7336 was in reasonable agreement with the Adj. R-Squared of 0.8867. Signal-to-noise ratio was 12.053, indicating an adequate signal. The linear coefficients of the cocatalyst (B) and the cross-product coefficients of catalyst×moderator (AC) were significant. The response surface and contour curves were obtained using Eq. (5):

$$\begin{aligned}\textbf{PolyDCPD conversion} = {} & +94.77 - 0.15\times\text{Catalyst} - 5.05\times\text{Cocatalyst} \\ & +0.65\times\text{Moderator} + 2.38\times\text{Catalyst} \\ & \times\text{Moderator} - 1.25\times\text{Catalyst}^2 - 1.40 \\ & \times\text{Cocatalyst}^2 + 0.46\times\text{Moderator}^2\end{aligned} \quad (5)$$

where cocatalyst is a linear factor having a positive effect on PolyDCPD conversion. The catalyst and moderator interacted with each other in PolyDCPD Conversion. Fig. 4(a) shows how the amount of catalyst and cocatalyst affected PolyDCPD conversion with constant moderator. PolyDCPD conversion was increased up to 98.3%, which was beneficial because a higher conversion allowed all DCPD to be involved in the ROMP reaction. PolyDCPD conversion appeared to depend largely on the cocatalyst rather than the catalyst. If the catalyst amount was too small or too large, the PolyDCPD conversion became somewhat low. PolyDCPD conversion was adjusted from 87% to 97% when the catalyst was 1 (DCPD/catalyst=1000, see Table 2) or −1 (DCPD/catalyst=3000), in accordance with the cocatalyst content, and from 88% to 98.3% when the catalyst was about 0 (DCPD/Catalyst=2000) according to the cocatalyst content. The highest value was 98.3% and the conditions were (0, −1, 0); i.e., DCPD/Catalyst=2000, DCPD/Cocatalyst=1000, DCPD/Moderator=400. Fig. 4(b), (c) shows the effect of moderator on PolyDCPD conversion. In Fig. 4(b) PolyDCPD conversion decreased from 96% to 92% as the moderator increased when the catalyst was −1 (DCPD/catalyst=3000) and increased from 90% to 97% when catalyst was 1 (DCPD/catalyst= 1000). As mentioned in Eq. (5), the catalyst and the moderator interact with each other. In Fig. 4(b) when the amount of catalyst was small (~−1), the conversion of PolyDCPD was slightly reduced as the moderator decreased, while when the amount of catalyst was high (~1), the PolyDCPD conversion increased more significantly as the moderator decreased. In Fig. 4(c) PolyDCPD conversion was nearly maintained from 88% to 89% as the moderator increased when cocatalyst was −1 (DCPD/cocatalyst=1000) and increased a little from 98% to 99.6% when cocatalyst was 1 (DCPD/cocatalyst=250)

5. PolyDCPD RIM Process Optimization

The optimal combination that satisfies each response range was obtained by using the optimization program BBD. Fig. 5 shows the optimum values (dashed area) of the catalyst and the cocatalyst according to the amount of moderator in the PolyDCPD RIM process. If the moderator was less than 0.2 (DCPD/Moderator= 340), the optimum value was not obtained (Fig. 5(a)). This was because a small amount of moderator failed to control the cocatalyst function being the reaction rate control so conversion was reduced due to the rapid reaction. Despite an increase in moderator (DCPD/moderator=100), when the catalyst amount was less than 0 (DCPD/catalyst=2000) the optimum value was not attained.

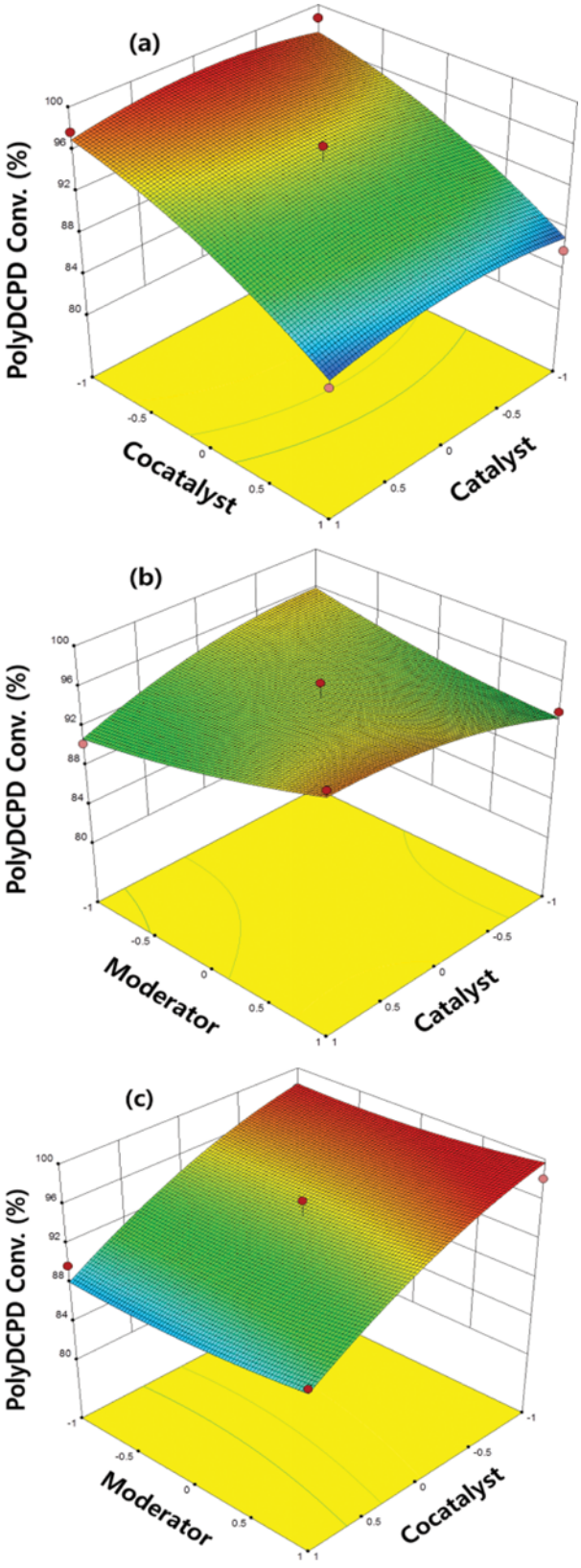

Fig. 4. Response surface plot of PolyDCPD conversion in the DCPD RIM process (a) with constant moderator (coded level=0, DCPD/moderator=400), (b) with constant cocatalyst (coded level=0, DCPD/cocatalyst=500), and (c) with constant catalyst (coded level=0, DCPD/catalyst=1000).

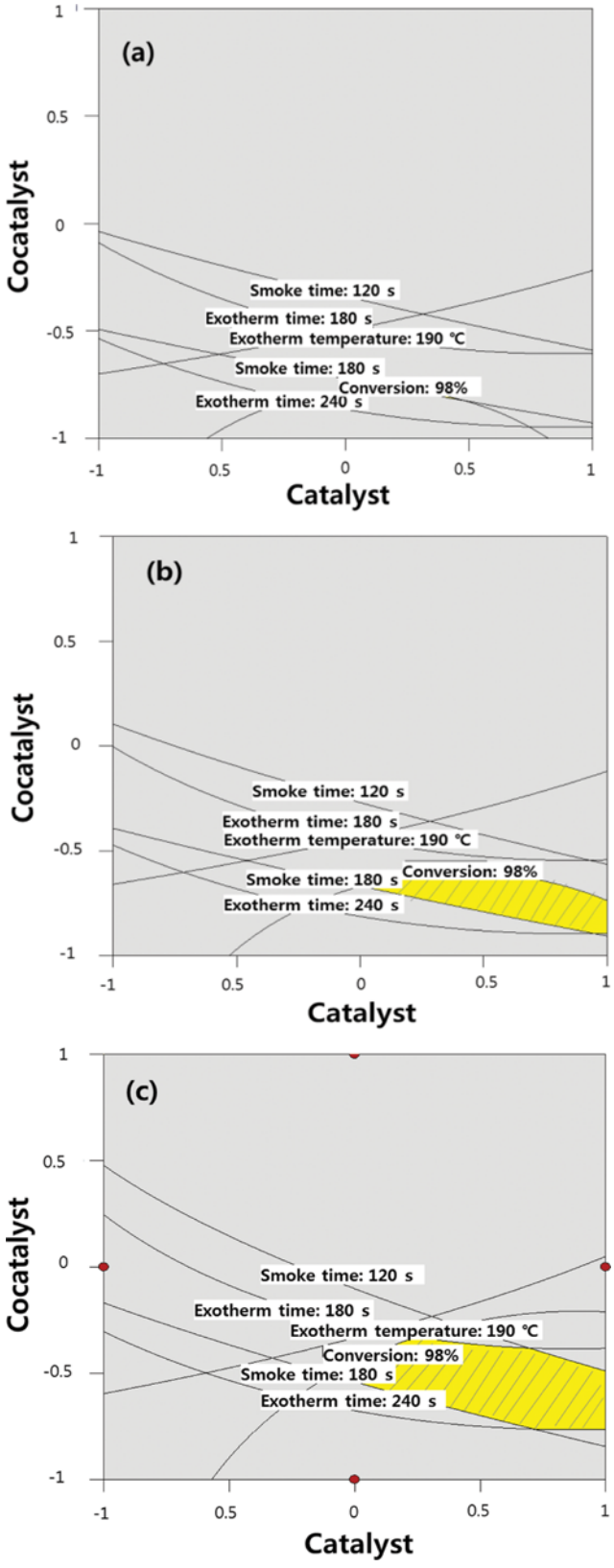

Fig. 5. Optimal catalyst and cocatalyst composition (dashed area) in the DCPD RIM process (a) when the moderator value is 0.2 (DCPD/moderator=340), (b) when the moderator value is 0.5 (DCPD/moderator=250), and (c) when the moderator value is 1.0 (DCPD/moderator=100).

Table 8. Physical properties of the PolyDCPD standard specimen with a composition in the processing region

Variables (mole ratio)	(a) Coded level (−0.1, −0.5, 1.0)	(b) Coded level (0.2, −0.6, 1.0)	(c) Coded level (0.5, −0.6, 1.0)
DCPD/catalyst	1/2100	1/1800	1/1500
DCPD/cocatalyst	1/750	1/800	1/800
DCPD/moderator	1/100	1/100	1/100
DCPD/stabilizer	1/2100	1/1800	1/1500
Tensile modulus (GPa)	1.49	1.55	1.43
Tensile strength (MPa)	35.9	40.5	33.9
Flexural modulus (GPa)	1.80	1.85	1.74
Flexural strength(MPa)	51.3	60.1	45
Impact strength (kJ/m^2)	60.3	69.0	59.6

This could be deduced based on the optimum conditions for smoke time, as well as the time to exotherm that moved into the area of high amount of the cocatalyst (left side of Fig. 5(b), (c)). This could be explained by the fact that the catalyst amount was too small for the catalyst to be fully activated by a cocatalyst; therefore, the polyDCPD conversion and exotherm temperature were low. However, when the amount of catalyst was greater than 0 (DCPD/catalyst= 2000) and that of the moderator close to 1 (DCPD/Moderator= 100), the PolyDCPD conversion could be expanded to conditions allowing varying amounts of cocatalyst to be used (right side of Fig. 5(b), (c)). This resulted in the optimal value becoming a large area. From the viewpoint of the catalyst and cocatalyst, the use of lower amounts of catalyst (Fig. 5(a), (b), (c); upper left) caused the reaction to become faster and the maximum temperature to be reached sooner (smoke time<100 s and exotherm time<180 s), which were not the optimum conditions. Using a larger amount of catalyst (Fig. 5(a), (b), (c); right below) caused the reaction to be more stable. In this case, increasing the amount of moderator (Fig. 5(b) and Fig. 5(c)) reduces the rate at which the catalyst initiates. As a result, the process optimization was expanded in accordance with an increase in PolyDCPD conversion area. The physical properties of the specimen were measured in three cases, and are shown in Table 8, in which (a), (b) and (c) correspond to the process optimum conditions. Among them, (b) condition could be described as good physical properties as well as optimum RIM process conditions. The optimum values obtained by RSM do not correspond to the optimum physical properties, but represent the optimum values of the RIM process, which do not affect the final properties. However, it is possible to improve the physical properties by mixing the composition within the optimum values. The region that does not correspond to the optimum value (dashed area) in the half circle of the conversion (Fig. 5(c)) indicates good properties since the physical properties depend on the conversion. However, in this case, either the process could take a long time or the material could harden before entering the mold. Moreover, it is difficult to obtain good physical properties in the section outside the optimum range due to the low conversion.

CONCLUSION

The response of the RIM process for the formulation of PolyDCPD by ROMP of the petrochemical by-product DCPD can be represented as a 3D graph using BBD. In addition, by setting the response range that can be used in the actual RIM process, the optimal parameter range was obtained, and the properties were measured using these conditions. The response changes for smoke time, exotherm temperature and PolyDCPD conversion with variables such as the amounts of catalyst, cocatalyst, and moderator were calculated using the BBD. Almost all responses were greatly affected by the cocatalyst. The range of each response for the DCPD RIM process was set and the optimum process conditions to satisfy all responses were determined. Optimal conditions had a significant effect on the cocatalyst/catalyst molar ratio. A large area of optimal values was obtained with a small cocatalyst/catalyst molar ration (1.5-3.0) and a large amount of moderator (DCPD/Moderator~100) used to adjust the performance of the cocatalyst. Therefore, it was possible to select many variables corresponding to the optimum value area. We also measured the physical properties (tensile, flexural, impact strength) of the specimen by applying three optimum conditions. The optimum value of coded level (0.4, –0.5, 1.0) was sufficient to fulfill the RIM process and physical properties of car exterior parts.

ACKNOWLEDGEMENTS

This study was supported by the Korea Research Institute of Chemical Technology program (SI-1709-01).

REFERENCES

1. L. W. Cheah, *Cars on a Diet: The Material and Energy Impacts of Passenger Vehicle Weight Reduction in the U.S*, Doctoral Thesis, Massachusetts Institute of Technology (2010).
2. N. Lutsey, *Review of technical literature and trends related to automobile mass-reduction technology*, Institute of Transportation Studies, University of California (2010).
3. R. Sinha, D. D. Pelot, Z. P. Zhou, A. Rahman, X. F. Wu and A. L. Yarin, *J. Mater. Chem.*, **22**, 9138 (2012).
4. F. Hu, J. Du and Y. Zheng, *Polym. Compos.*, **35**, 1918 (2014).
5. J. C. Mol, *J. Mol. Catal. A: Chem.*, **213**, 39 (2004).
6. M. E. Jamróz, S. Gałka and J. C. Dobrowolski, *J. Mol. Struct. Theochem.*, **634**, 225 (2003).

7. H. Li, Z. Wang and B. He, *J. Mol. Catal. A: Chem.*, **147**, 83 (1999).
8. W. Shan and Y. Mei, *Polym. Sci. Ser. B*, **55**, 344 (2013).
9. H. C. Hsu, S. J. Wang, J. D. Y. Ou and D. S. H. Wong, *Ind. Eng. Chem. Res.*, **54**, 9798 (2015).
10. C. Bergström, J. Koskinen, E. Halme, M. Lindström and M. Perälä, US Patent, 6,294,706B1 (2001).
11. J. D. Rule and J. S. Moore, *Macromolecules*, **35**, 7878 (2002).
12. J. J. Zou, X. Zhang, J. Kong and L. Wang, *Fuel*, **87**, 3655 (2008).
13. T. J. Bruno, M. L. Huber, E. W. Lemmon and R. A. Perkins, *Thermophysical Properties of JP-10*, National Institute of Standards and Technology (2006).
14. E. Xing, X. Zhang, L. Wang and Z. Mi, *Green Chem.*, **9**, 589 (2007).
15. Special Reports, *Opportunities in C5 Chemicals: A Business Analysis prospectus*, NexantThinking™ (http://thinking.nexant.com/) (2014).
16. *C5 Value Chain Study: From Cracker to Key C5 Derivative Applications for Isoprene, DCPD and Piperylene*, IHS Chemical, Special Report Prospectus (2015).
17. Global Polydicyclopentadiene (PDCPD) Industry Report 2016, QYR Chemical & Material Research Center (2016).
18. M. Takahiro, *The latest technologies and applications of RIM molding (DCPD)*, Plastic Age (2008).
19. Sojitz New Release, July 8, Sojitz corporation, (https://www.sojitz.com/en/news/yearly/2008/) (2008).
20. M. N. Bogomolova, D. I. Zemlyakov, N. I. Sidorenko, R. V. Ashirov, D. A. Rusakov and V. K. Chaikovskii, *Int. Polymer Sci. Technol.*, **40**, 7 (2012).
21. Z. Yao, L. Zhou, B. Dai and K. Cao, *J. Appl. Polym. Sci.*, **125**, 2489 (2012).
22. R. H. Grubbs, *Tetrahedron*, **60**, 7117 (2004).
23. S. Doughty, G. Recher and Y. S. Yang, *Kunstst. Ger. Plast.*, **82**, 12 (1992).
24. R. M. Elder, J. W. Andzelm and T. W. Sirk, *Chem. Phys. Lett.*, **637**, 103 (2015).
25. L. Gong, K. Liu, E. Ou, F. Xu, Y. Lu, Z. Wang, T. Gao, Z. Yang and W. Xu, *RSC Adv.*, **5**, 26185 (2015).
26. E. J. Lee, H. S. Kim, B. K. Lee, W. S. Hwang, I. K. Sung and I. M. Lee, *Bull. Korean Chem. Soc.*, **33**, 4131 (2012).
27. S. Kovacic, *Acta Chim. Slov.*, **60**, 448 (2013).
28. C. H. Hong, S. W. Song, B. U. Nam, B. J. Cha and B. J. Kim, *Polym-Korea*, **30**, 311 (2006).
29. E. A. Ofstead and N. Calderon, *Makromol. Chem.*, **154**, 21 (1972).
30. A. J. Amass, M. Lotfipour, J. A. Zurimendi, B. J. Tighe and C. Thompson, *Makromol. Chem.*, **188**, 2121 (1987).
31. R. W. Layer, US Patent, 4,484,010 (1993).
32. N. Ledoux, *Ruthenium Olefin Metathesis Catalysts: Tuning of the Ligand Environment, Promotor*, Doctoral Thesis, Universiteit Gent (2007).
33. W. Jeong and M. R. Kessler, *Chem. Mater.*, **20**, 7060 (2008).
34. S. Bluestone, S. D. Heister and S. F. Son, 46th AIAA/ASME/SAE/ASEE Joint Propulsion Conference & Exhibit, Nashville, TN, 1 (2010).
35. J. I. Kroschwitz and M. Howe-Grant, *Encyclopedia of Chemical Technology*, Wiley Interscience, New York, **17**, 829 (1996).
36. D. D. Andjelkovic and R. C. Larock, *Biomacromolecules*, **7**, 927 (2006).
37. W. S. Kong, T. J. Ju and J. H. Park, *Int. J. Adhes. Adhes.*, **38**, 7 (2012).
38. A. Teixeira and B. Ribeiro, Rapid Product Development, 1 (2010).
39. S. Monsaert, N. Ledoux, R. Drozdzak and F. Verpoort, *J. Polym. Sci., Part A: Polym. Chem.*, **48**, 302 (2010).
40. D. W. Klosiewicz, US Patent, 4,520,181 (1985).
41. D. Astruc, *New J. Chem.*, **29**, 42 (2005).
42. D. R. Kelsey, D. L. Handlin, Jr. M. Narayana and B. M. Scardino, *J. Polym. Sci., Part A: Polym. Chem.*, **35**, 3027 (1997).
43. Y. S. Yang, E. Lafontaine and B. Mortaigne, *Polymer*, **38**, 1121 (1997).
44. D. Gangadharan, S. Sivaramakrishnan and K. M. Nampoothiri, *Bioresour. Technol.*, **99**, 4597 (2008).
45. M. Hasan Beikdashti, H. Forootanfar, M. S. Safiarian, A. Ameri, M. H. Ghahremani, M. R. Khoshayand and M. A. Faramarzia, *J. Taiwan Inst. Chem. Eng.*, **43**, 670 (2012).
46. G. E. P. Box and D. W. Behnken, *Technometrics*, **2**, 455 (1960).
47. D. C. Montogomery, *Design and Analysis of Experiments*, Wiley, New York (2001).
48. K. Singh, G. Srivastava, M. Talat, O. N. Srivastava and A. M. Kayastha, *Biophys. Rep.*, **3**, 18 (2015).
49. C. H. Ali, S. M. Mbadinga, J. F. Liu, S. Z. Yang, J. D. Gu and B. Z. Mu, *J. Taiwan Inst. Chem. Eng.*, **52**, 7 (2015).
50. A. J. Jafari, B. Kakavandi, R. R. Kalantary, H. Gharibi, A. Asadi, A. Azari, A. A. Babaei and A. Takdastan, *Korean J. Chem. Eng.*, **33**, 2878 (2016).
51. L. Chen, P. Yin, R. Qu, X. Chen, Q. Xu and Q. Tang, *Chem. Eng. J.*, **173**, 583 (2011).
52. D. W. Klosiewicz, US Patent, 4,400,340 (1983).
53. A. E. Martin, US Patent, 4,918,039 (1988).
54. Y. S. Yang, E. Lafontaine and B. Mortaigne, *Polymer*, **38**, 1121 (1997).
55. P. Y. Le Gaca, D. Choqueusea, M. Parisb, G. Recherc, C. Zimmerd and D. Melote, *Polym. Degrad. Stab.*, **98**, 809 (2013).